Materials Science and Engineering B 175 (2010) 261–265

Contents lists available at ScienceDirect

Materials Science and Engineering B

journal homepage: www.elsevier.com/locate/mseb

Preparation of $PtSnO_2$/C electrocatalysts using electron beam irradiation

Dionísio F. Silva[a], Adriana N. Geraldes[a], Almir Oliveira Neto[a], Eddy S. Pino[a], Marcelo Linardi[a], Estevam V. Spinacé[a,*], Waldemar A.A. Macedo[b], José D. Ardisson[b]

[a] Instituto de Pesquisas Energéticas e Nucleares (IPEN-CNEN/SP), Av. Professor Lineu Prestes 2242, 05508-900 São Paulo, SP, Brazil
[b] Serviço de Nanotecnologia, Centro de Desenvolvimento da Tecnologia Nuclear (CDTN), 31270-901 Belo Horizonte, MG, Brazil

ARTICLE INFO

Article history:
Received 26 April 2010
Received in revised form 7 July 2010
Accepted 28 August 2010

Keywords:
Platinum
SnO_2
Electrocatalyst
Electron beam
Ethanol
Fuel cell

ABSTRACT

$PtSnO_2$/C electrocatalysts with Pt:Sn atomic ratios of 75:25, 50:50 and 25:75 were prepared in water/2-propanol using electron beam irradiation. The materials were characterized by energy-dispersive X-ray analysis, X-ray diffraction, Mössbauer spectroscopy and transmission electron microscopy. The electro-oxidation of ethanol was studied by chronoamperometry at room temperature and on direct ethanol fuel cell (DEFC) at 100 °C. The X-ray diffraction and Mössbauer measurements of the $PtSnO_2$/C electrocatalysts showed typical face-centered cubic (fcc) structure of platinum and the presence of a SnO_2 phase (cassiterite). The $PtSnO_2$/C electrocatalysts were active for ethanol electro-oxidation and the material with Pt:Sn atomic ratio of 50:50 showed the best performance.

1. Introduction

Fuel cells convert chemical energy directly into electrical energy with high efficiency and are extremely attractive as power sources for mobile, stationary and portable applications [1]. However, the use of hydrogen as combustible continues to present problems especially for mobile and portable applications [2]. Thus, there has been an increasing interest in the use of alcohols directly as combustible (Direct Alcohol Fuel Cell—DAFC). Methanol has been considered the most promising alcohol and carbon-supported PtRu nanoparticles (PtRu/C electrocatalyst) the best electrocatalyst [3]. In Brazil ethanol is an attractive fuel as it is produced in large quantities from sugar cane and it is much less toxic than methanol, however, its complete oxidation to CO_2 is more difficult than that of methanol due to the difficulty in C–C bond breaking and to the formation of CO-intermediates that poison the platinum anode catalysts [4–6]. Thus, more active electrocatalysts are essential to enhance the ethanol electro-oxidation. PtSn-based electrocatalysts have been shown good performances for ethanol electro-oxidation [6,7]. Depending on the preparation procedure PtSn/C electrocatalysts have been obtained with different particle sizes and surface composition. Moreover, Sn could be found as PtSn alloys and/or in a non-alloyed oxidized state (SnO_x). Considering that the chemical and physical characteristics of these electrocatalysts depend on the preparation procedure, the way of preparation becomes a key factor regarding their electrochemical activity [6]. Thus, until now, the optimum Sn content in the PtSn electrocatalysts has not been determined because it depends on the intrinsic characteristics of the obtained material [6].

Active carbon-supported metal nanoparticles for fuel cell applications has been prepared by radiation-induced reduction of metal ions precursors [8–12]. We prepared PtRu/C electrocatalysts for methanol oxidation using gamma and electron beam irradiation [13–15]. Using electron beam irradiation, active PtRu/C electrocatalysts could be prepared within few minutes of irradiation [15]. In this work, $PtSnO_2$/C electrocatalysts with different Pt:Sn atomic ratios were prepared in water/2-propanol using electron beam irradiation. The obtained materials were tested for ethanol electro-oxidation.

2. Experimental

$PtSnO_2$/C electrocatalysts (20 wt% of metal loading) were prepared with different Pt:Sn atomic ratios using $H_2PtCl_6{\cdot}6H_2O$ (Aldrich) and $SnCl_2{\cdot}2H_2O$ (Aldrich) as metal sources, which were dissolved in water/2-propanol solution 50/50 (v/v). After this, the Carbon Vulcan® XC72R, used as support, was dispersed in the solution using an ultrasonic bath. The resulting mixtures were submitted (at room temperature and open atmosphere) under stirring to electron beam irradiation (Electron Accelerator's Dynamitron Job 188–IPEN/CNEN–SP) and the total dose applied was 288 kGy (dose rate 1.6 kGy s^{-1}, time 3 min). After electron beam irradiation, the

* Corresponding author. Tel.: +55 11 31339284; fax: +55 11 31339193.
E-mail address: espinace@ipen.br (E.V. Spinacé).

0921-5107/$ – see front matter © 2010 Elsevier B.V. All rights reserved.
doi:10.1016/j.mseb.2010.08.002

mixtures were filtered and the solids ($PtSnO_2$/C electrocatalysts) were washed with water and dried at 70 °C for 2 h [13–15].

The Pt:Sn atomic ratios were obtained by energy-dispersive X-ray analysis (EDX) using a Philips XL30 scanning electron microscope with a 20 keV electron beam and provided with EDAX DX-4 microanalizer.

The X-ray diffraction (XRD) analyses were carried out in a Miniflex II model Rigaku diffractometer using Cu Kα radiation (λ = 0.15406 nm). The diffractograms were recorded at 2θ in the range 20–90° with step size of 0.05° and scan time of 2 s per step. The average crystallite size was calculated using Scherrer equation [16].

Transmission electron microscopy (TEM) was carried out using a JEOL JEM-2100 electron microscope operated at 200 kV. The particle distribution histogram was determined by measuring 150 particles from micrograph.

The ^{119}Sn Mössbauer experiments were performed employing a conventional constant acceleration spectrometer and a source of ^{119m}Sn in a $CaSnO_3$ matrix. The samples were kept at 77 K inside a closed cycle helium cryostat with the $CaSnO_3$ source at room temperature. All spectra were computer-fitted assuming Lorentzian lines.

Electrochemical studies of the electrocatalysts were carried out using the thin porous coating technique [17]. An amount of 20 mg of the electrocatalyst was added to a solution of 50 mL of water containing 3 drops of a 6% polytetrafluoroethylene (PTFE) suspension. The resulting mixture was treated in an ultrasound bath for 10 min, filtered and transferred to the cavity (0.30 mm deep and 0.36 cm^2 area) of the working electrode. The reference electrode was a RHE and the counter electrode was a platinized Pt plate. Electrochemical measurements were made using a Microquimica (model MQPG01, Brazil) potentiostat/galvanostat. Cyclic voltammetry was performed using 1.0 mol L^{-1} of ethanol in 0.5 mol L^{-1} H_2SO_4 solution saturated with N_2. Chronoamperometry experiments were performed using 1.0 mol L^{-1} of ethanol in 0.5 mol L^{-1} H_2SO_4 at 0.5 V and at room temperature. For comparative purposes a commercial PtSn/C BASF electrocatalyst (20 wt%, Pt:Sn atomic ratio of 3:1, alloy, Lot #F0930203) was used.

The membrane electrode assemblies (MEA) were prepared by hot pressing a pretreated Nafion 117 membrane placed between either a commercial PtSn/C BASF or $PtSnO_2$/C prepared in this work as anode (1 mg Pt cm^{-2} catalyst loading) and a 20 wt% Pt/C E-TEK cathode (1 mg Pt cm^{-2} catalyst loading) at 125 °C for 2 min under a pressure of 225 kgf cm^{-2}. The direct ethanol fuel cell performances were determined in a single cell with an area of 5 cm^2. The temperature was set to 100 °C for the fuel cell and 80 °C for the oxygen humidifier. The fuel was 2 mol L^{-1} ethanol solution delivered at approximately 2 mL min^{-1} and the oxygen flow was regulated at 500 mL min^{-1} and pressure of 2 bar. Polarization curves were obtained by using a TDI RBL 488 electronic load.

3. Results and discussion

Electron beam irradiation of a water solution causes the ionization and excitation of water molecules producing the species shown in Eq. (1) [9]:

$$H_2O \rightarrow e_{aq}^-, H^+, H^\bullet, OH^\bullet, H_2O_2, H_2 \quad (1)$$

The solvated electrons, e_{aq}^-, and H• atoms are strong reducing agents and were able to reduce metal ions down to the zero-valent state (Eqs. (2) and (3)):

$$M^+ + e_{aq}^- \rightarrow M^0 \quad (2)$$

$$M^+ + H^\bullet \rightarrow M^0 + H^+ \quad (3)$$

Table 1
Pt:Sn atomic ratios and crystallite sizes of the $PtSnO_2$/C electrocatalysts prepared with different Pt:Sn atomic ratios using electron beam irradiation.

Pt:Sn atomic ratio (nominal)	Pt:Sn atomic ratio (EDX)	Crystallite size (nm)
25:75	32:68	3.2
50:50	51:49	3.0
75:25	69:31	3.3

On the other hand, OH• radicals could oxidize the ions or the atoms into a higher oxidation state and thus to counterbalance the reduction reactions (2) and (3). Thus, an OH• radical scavenger is added to the solution, in this case 2-propanol, which reacts with these radicals leading to the formation of radicals exhibiting reducing power that are able to reduce metal ions (Eqs. (4) and (5)) [9]:

$$(CH_3)_2CHOH + {}^\bullet OH \rightarrow (CH_3)_2COH + H_2O \quad (4)$$

$$M^+ + (CH_3)_2COH \rightarrow M^0 + (CH_3)_2CO + H^+ \quad (5)$$

In this manner, the atoms produced by the reduction of metals ions progressively coalesce leading to the formation of the metal nanoparticles.

The $PtSnO_2$/C electrocatalysts prepared with different Pt:Sn atomic ratios using electron beam irradiation are shown in Table 1. For all samples, Pt:Sn atomic ratios determined by EDX analysis were similar to the nominal ones. After separation of the obtained $PtSnO_2$/C electrocatalysts by filtration, a qualitative test using potassium iodide [18] did not detect Pt ions in the filtrates, which suggest that all Pt(IV) ions were reduced to metallic Pt. As no Pt ions were not detected in the filtrates and the obtained Pt:Sn atomic ratios were similar to the nominal ones, it was considered that all electrocatalysts were obtained with 20 wt% of metal loading.

The XRD diffratograms of Pt/C and $PtSnO_2$/C electrocatalysts (Fig. 1) showed a broad peak at about 25°, which was associated to the Vulcan XC72R support material, and five diffraction peaks at about 2θ = 40°, 47°, 67°, 82°, and 87° that are associated to the (1 1 1), (2 0 0), (2 2 0), (3 1 1) and (2 2 2) planes, respectively, which are characteristic of the fcc structure of platinum and platinum alloys [19]. The (2 2 0) reflections of the Pt fcc structure were used to calculate the average crystallite size according to Scherrer formula [16] and the values were in the range of 3.0–3.5 nm (Table 1). For comparative purposes it is shown in Fig. 1 the diffractogram of the commercial PtSn/C BASF electrocatalyst (PtSn alloy). In this case, it was observed a shift of the peaks relative to Pt(fcc) phase to lower angles compared to those of Pt/C electrocatalyst. This shift was not observed for all $PtSnO_2$/C electrocatalysts showing

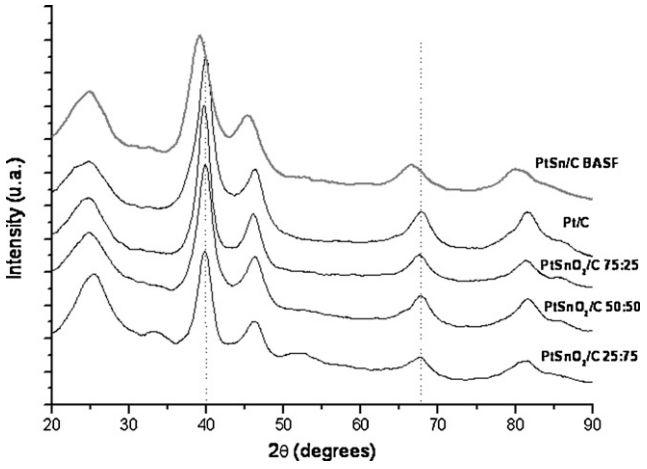

Fig. 1. X-ray diffractograms of Pt/C and $PtSnO_2$/C electrocatalysts prepared using electron beam irradiation.

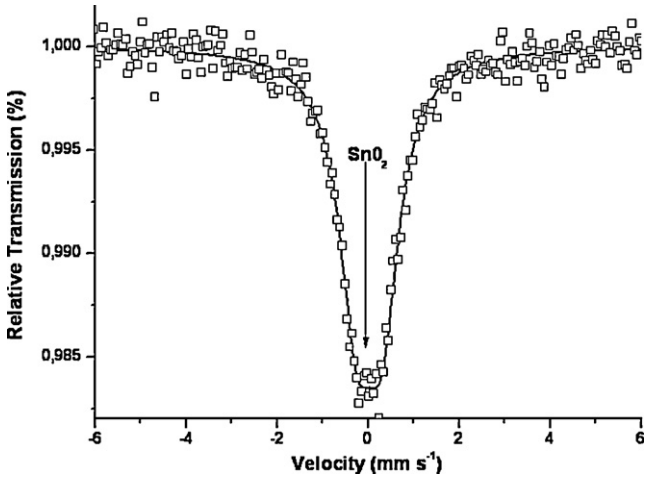

Fig. 2. Mössbauer spectra of the $PtSnO_2$/C electrocatalyst prepared with Pt:Sn atomic ratio of 50:50.

that no PtSn alloys were formed. However, two peaks at approximately $2\theta = 34^\circ$ and 52° were observed in the diffractogram of the $PtSnO_2$/C electrocatalyst prepared with Pt:Sn atomic ratio of 25:75, which were identified as a SnO_2 phase (cassiterite) [7,20,21]. The X-ray diffractogram of the cassiterite SnO_2 phase showed the most intense peaks at about $2\theta = 27^\circ$, 34° and 52° [21]. The peak at $2\theta = 27^\circ$ was not observed in the diffractogram of $PtSnO_2$/C electrocatalyst prepared with Pt:Sn atomic ratio of 25:75, which could be due to the broad peak of the carbon support at about $2\theta = 25^\circ$. Besides, the peaks of the SnO_2 phase were not clearly seen in the diffractograms of PtSn/C electrocatalysts prepared with Pt:Sn atomic ratios of 75:25 and 50:50 probably due the low intensities and broadness of the peaks. The presence of SnO_2 phase on these electrocatalysts was observed by Mössbauer spectroscopy. The ^{119}Sn Mössbauer spectrum of the $PtSnO_2$/C electrocatalyst prepared with Pt:Sn atomic ratio of 50:50 is shown in Fig. 2. It consisted of a broad peak centered near zero velocity that is typical of Sn(IV) and can be assigned to SnO_2 (the typical quadrupole doublet of cassiterite). No peaks of Pt_3Sn, PtSn, SnO and Sn(0) species were observed in the spectrum [22,23]. Thus, from Mössbauer and XRD measurements it can be concluded that Pt(fcc) and a SnO_2 phases coexist in the obtained electrocatalysts. Henglein and Giersig [24] described the preparation of colloidal Sn by radiolytic reduction of $SnCl_2$ in water/2-propanol. In this case, all process steps were performed under controlled argon atmosphere. In our case, the experiments were performed in open atmosphere and the SnO_2 phase was probably formed through hydrolysis–oxidation of $SnCl_2$ [25]. Thus, only Pt(IV) ions were reduced to metallic Pt under the used conditions.

TEM micrograph and the corresponding particle size distribution histogram of the $PtSnO_2$/C electrocatalyst prepared with Pt:Sn atomic ratio of 50:50 are shown in Fig. 3a and b, respectively. It can been seen that the nanoparticles were homogeneously distributed on the carbon support and the mean particle size was 2.7 nm.

The cyclic voltammograms (CV) of $PtSnO_2$/C electrocatalysts in 0.5 mol L^{-1} H_2SO_4 containing 1.0 mol L^{-1} of ethanol are shown in Fig. 4. The current values were normalized per gram of platinum, considering that ethanol adsorption and dehydrogenation occur only on platinum sites at room temperature [26]. The electrooxidation of ethanol started at low potential (around 0.2–0.3 V) for all electrocatalysts. $PtSnO_2$/C eletrocatalysts prepared with Pt:Sn atomic ratio of 50:50 and 75:25 showed similar performance in the region of 0.3–0.5 V and above 0.5 V the material prepared with Pt:Sn atomic ratio of 50:50 showed higher oxidation current values than the other ones.

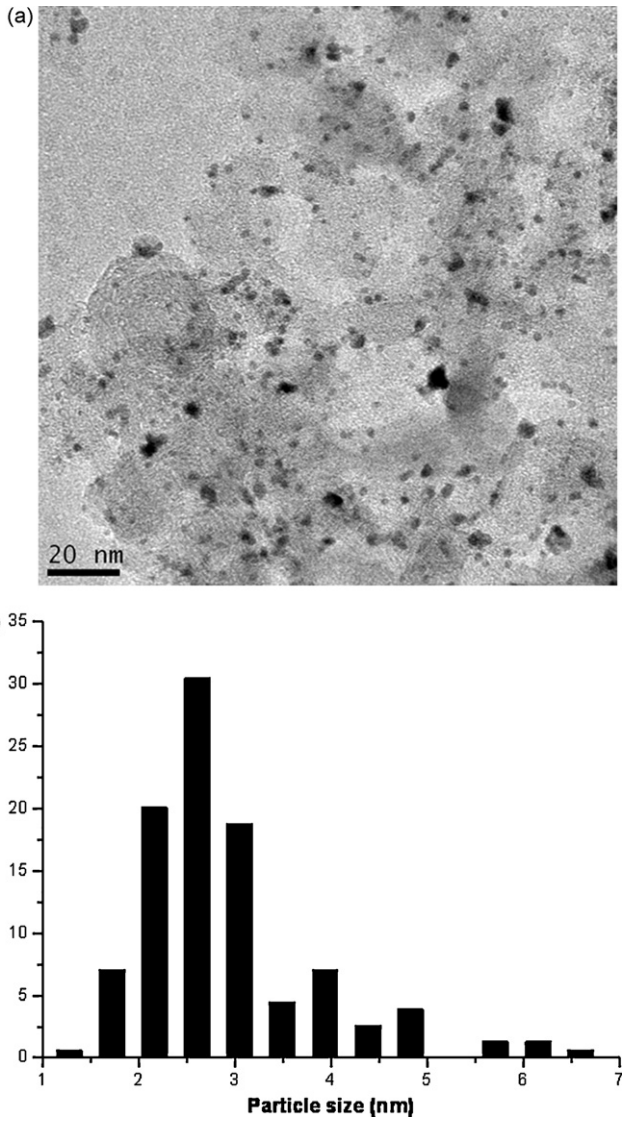

Fig. 3. (a) TEM micrograph and (b) particle size distribution of $PtSnO_2$/C electrocatalyst prepared with Pt:Sn atomic ratio of 50:50.

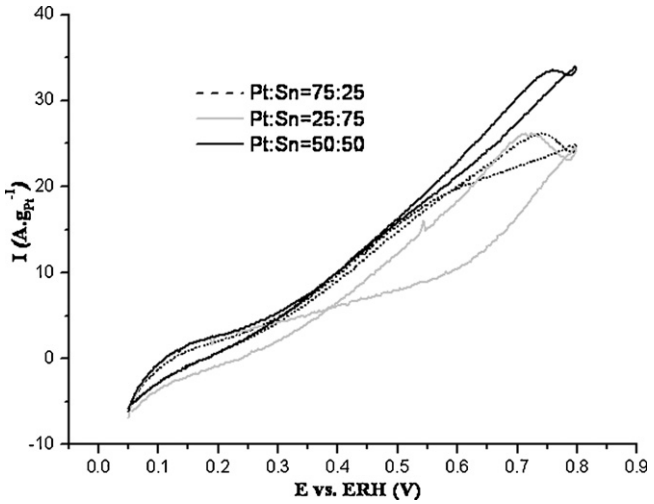

Fig. 4. Cyclic voltammetry of $PtSnO_2$/C electrocatalysts in 0.5 mol L^{-1} H_2SO_4 containing 1.0 mol L^{-1} ethanol with a sweep rate of 10 mV s^{-1}.

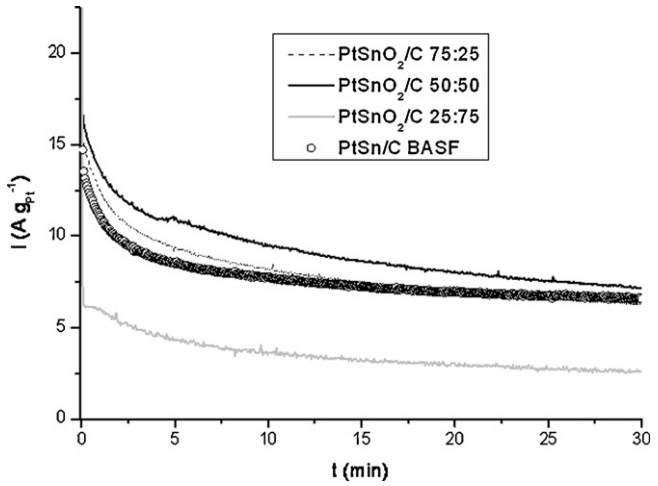

Fig. 5. Current–time curves at 0.5 V for $PtSnO_2$/C electrocatalysts in 1.0 mol L^{-1} ethanol in 0.5 mol L^{-1} H_2SO_4.

The chronoamperometric curves of $PtSnO_2$/C electrocatalysts in 1 mol L^{-1} ethanol in 0.5 mol L^{-1} H_2SO_4 at 0.5 V for 30 min are shown in Fig. 5. In all current–time curves there is an initial current drop in the first minutes followed by a slower decay. The following order of activity for ethanol oxidation was observed: 50:50 > 75:25 ≫ 25:75. In comparison to the commercial PtSn/C BASF electrocatalyst the material prepared with Pt:Sn atomic ratio of 50:50 showed a superior performance while the material prepared with 75:25 showed a similar behavior.

Fig. 6 shows the performances of single cell with commercial PtSn/C BASF and $PtSnO_2$/C prepared with Pt:Sn atomic ratio of 50:50 as anode electrocatalysts. The open circuit voltage of the fuel cell using $PtSnO_2$/C electrocatalyst was 0.66 V, while the corresponding value for PtSn/C BASF electrocatalyst was 0.65 V. The maximum power density of $PtSnO_2$/C electrocatalyst (35 mW cm^2) was similar to the obtained using the commercial electrocatalyst (37 mW cm^2). Despite of the commercial PtSn/C BASF (PtSn alloy) and the prepared $PtSnO_2$/C electrocatalyst has different Pt:Sn atomic ratios and chemical species, these electrocatalysts showed good performances for ethanol electro-oxidation. Similar results were described in the literature showing that $PtSnO_2$/C [6,7,20,27–32] and PtSn/C with a high degree of alloying [33–37] are

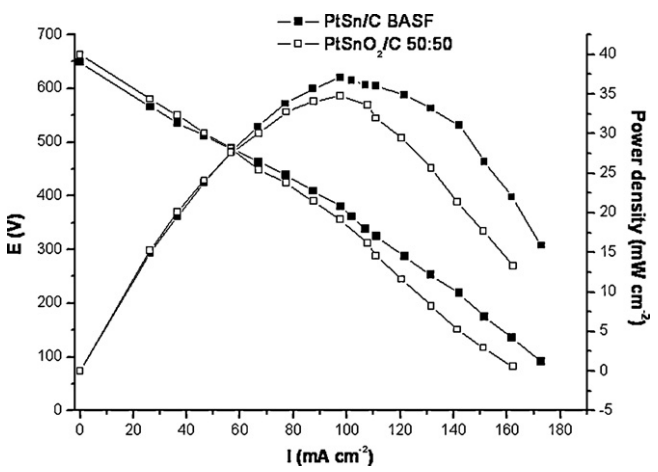

Fig. 6. *I–V* curves of a 5 cm^2 DEFC and the power density at 100 °C using commercial PtSn/C BASF and $PtSnO_2$/C electrocatalysts as anodes (1 mg Pt cm^2 catalyst loading) and commercial Pt/C E-TEK electrocatalyst as cathode (1 mg Pt cm^2 catalyst loading, 20 wt% catalyst on carbon), Nafion® 117 membrane, ethanol (2.0 mol L^{-1}), oxygen pressure (2 bar).

good electrocatalysts for ethanol electro-oxidation. Zhu et al. [38] prepared carbon-supported Pt–Sn electrocatalysts using different processes and evaluated the electrocatalytic activity and the final products of ethanol electro-oxidation. For $PtSnO_2$/C electrocatalyst it was observed an enhancement of the yield of acetic acid, while for PtSn/C electrocatalysts (with different alloy degrees) it was observed an increase of acetaldehyde with the increase of the alloy degree. It was proposed that non-alloyed SnO_2 species oxidized the adsorbed poisonous intermediates of ethanol electro-oxidation to acetic acid by providing OH species, according to bi-functional mechanism, whereas PtSn alloy phase strengthened the electronic effect of PtSn/C catalyst and accelerated the rate of the dehydrogenation of ethanol to acetaldehyde [37].

4. Conclusions

Active $PtSnO_2$/C electrocatalysts for ethanol oxidation were obtained in a single step at room temperature within few minutes using electron beam irradiation. The $PtSnO_2$/C electrocatalysts showed the typical Pt (fcc) structure and a cassiterite SnO_2 phase. The average crystallite sizes of the Pt (fcc) phase were around 3 nm. The $PtSnO_2$/C electrocatalyst prepared with Pt:Sn atomic ratio of 50:50 showed the best activity for ethanol electro-oxidation. Further work is now necessary to elucidate the mechanism of ethanol electro-oxidation using these catalysts.

Acknowledgments

The authors thank FAPESP (Proc. no. 2007/08724-7), FINEP-$ProH_2$, CNPq and Fapemig for financial support. CTR and CCTM from IPEN/CNEN-SP are acknowledged for electron beam irradiations and TEM measurements.

References

[1] H. Wendt, E.V. Spinacé, A.O. Neto, M. Linardi, Quim. Nova 28 (2005) 1066–1075.
[2] L. Schlapbach, A. Zuettel, Nature 414 (2001) 353–358.
[3] H. Liu, C. Song, L. Zhang, J. Zhang, H. Wang, D.P. Wilkinson, J. Power Sources 155 (2006) 95–110.
[4] W.J. Zhou, W.Z. Li, S.Q. Song, Z.H. Zhou, L.H. Jiang, G.Q. Sun, Q. Xin, K. Poulianitis, S. Kontou, P. Tsiakaras, J. Power Sources 131 (2004) 217–223.
[5] S. Rousseau, C. Coutanceau, C. Lamy, J.-M. Léger, J. Power Sources 158 (2006) 18–24.
[6] E. Antolini, J. Power Sources 170 (2007) 1–12.
[7] E.V. Spinacé, L.A.I. do Vale, R.R. Dias, A.O. Neto, M. Linardi, Stud. Surf. Sci. Catal. 162 (2006) 617–624.
[8] B. Le Gratiet, H. Remita, G. Picq, M.O. Delcourt, J. Catal. 164 (1996) 36–43.
[9] J. Belloni, M. Mostafavi, H. Remita, J.-L. Marignier, M.-O. Delcourt, New J. Chem. 22 (1998) 1239–1255.
[10] S.-D. Oh, K.R. Yoon, S.-H. Choi, A. Gopalan, K.-P. Lee, S.-H. Sohn, H.-D. Kang, I.S. Choi, J. Non-Cryst. Solids 352 (2006) 355–360.
[11] H. Wang, X. Sun, Y. Ye, S. Qiu, J. Power Sources 161 (2006) 839–842.
[12] G.S. Chai, B. Fang, J.-S. Yu, Electrochem. Commun. 10 (2008) 1801–1804.
[13] E.V. Spinacé, A.O. Neto, M. Linardi, D.F. Silva, E.S. Pino, V.A. Cruz, Patent BR200505416-A.
[14] D.F. Silva, A.O. Neto, E.S. Pino, M. Linardi, E.V. Spinacé, J. Power Sources 170 (2007) 303–307.
[15] D.F. Silva, A.O. Neto, E.S. Pino, M. Brandalise, M. Linardi, E.V. Spinacé, Mater. Res. 10 (2007) 367–370.
[16] V. Radmilovic, H.A. Gasteiger, P.N. Ross, J. Catal. 154 (1995) 98–106.
[17] A.O. Neto, M.J. Giz, J. Perez, E.A. Ticianelli, E.R. Gonzalez, J. Electrochem. Soc. 149 (2002) A272–A279.
[18] H.G. Julsing, R.I. McCrindle, S. Afr. J. Chem. 53 (2000) 86–89.
[19] A.O. Neto, T.R.R. Vasconcelos, R.W.R.V. Silva, M. Linardi, E.V. Spinacé, J. Appl. Electrochem. 35 (2005) 193–198.
[20] A.O. Neto, R.R. Dias, M.M. Tusi, M. Linardi, E.V. Spinacé, J. Power Sources 166 (2007) 87–91.
[21] Z. Chen, J.K.L. Lai, C.H. Shek, H. Chen, J. Mater. Res. 18 (2003) 1289–1292.
[22] N. Nava, A. Montoya, T. Viveros, Mol. Phys. 100 (2002) 3173–3175.
[23] N. Nava, M.A. Morales, W. Vanoni, J.A. Toledo, E. Baggio-Saitovitch, T. Viveros, Hyperfine Interact. 134 (2001) 81–92.
[24] A. Henglein, M. Giersig, J. Phys. Chem. 98 (1994) 6931–6935.
[25] K. Ke, Y. Yamazaki, K. Waki, J. Nanosci. Nanotechnol. 9 (2009) 366–370.
[26] H.A. Gasteiger, N. Markovic, P.N. Ross, E.J. Carins, J. Electrochem. Soc. 141 (1994) 1795–1803.

[27] E.V. Spinacé, M. Linardi, A.O. Neto, Electrochem. Commun. 7 (2005) 365–369.
[28] A.O. Neto, M. Linardi, D.M. dos Anjos, G. Tremiliosi-Filho, E.V. Spinacé, J. Appl. Electrochem. 39 (2009) 1153–1156.
[29] A.O. Neto, L.A. Farias, R.R. Dias, M. Brandalise, M. Linardi, E.V. Spinacé, Electrochem. Commun. 10 (2008) 1315–1317.
[30] L. Jiang, G. Sun, Z. Zhou, S. Sun, Q. Wang, S. Yan, H. Li, J. Tian, J. Guo, B. Zhou, Q. Xin, J. Phys. Chem. B 109 (2005) 8774–8778.
[31] J. Mann, N. Yao, A.B. Bocarsly, Langmuir 22 (2006) 10432–10436.
[32] A. Kowal, M. Li, M. Shao, K. Sasaki, M.B. Vukmirovic, J. Zhang, N.S. Marinkovic, P. Liu, A.I. Frenkel, R.R. Adzic, Nat. Mater. 8 (2009) 325–330.
[33] R. Alcala, J.W. Shabaker, G.W. Huber, M.A. Sanchez-Castillo, J.A. Dumesic, J. Phys. Chem. B 109 (2005) 2074.
[34] X. Tang, B. Zhang, Y. Li, Y. Xu, Q. Xin, W. Shen, J. Mol. Catal. A: Chem. 235 (2005) 122.
[35] F. Colmati, E. Antolini, E.R. Gonzalez, Electrochim. Acta 50 (2005) 5496.
[36] R.F.B. De Souza, L.S. Parreira, D.C. Rascio, J.C.M. Silva, E. Teixeira-Neto, M.L. Calegaro, E.V. Spinace, A.O. Neto, M.C. Santos, J. Power Sources 195 (2010) 1589–1593.
[37] D.R.M. Godoi, J. Perez, H.M. Villullas, J. Power Sources 195 (2010) 3394–3401.
[38] M. Zhu, G. Suna, Q. Xin, Electrochim. Acta 54 (2009) 1511–1518.